

LIVE LOAD DISTRIBUTION FACTORS FOR SHEAR FORCE IN NEXT BEAM BRIDGES

Jianwei Huang, Ph.D., P.E., M.PCI, Assistant Professor, Department of Civil Engineering, Southern Illinois University Edwardsville. Edwardsville, IL

ABSTRACT

The PCI northeast bridge technical committee developed northeast extreme tee (NEXT) beam sections that would be good candidates for medium span bridges. The NEXT beams offered several advantages over other types of beams in several aspects, such as no intermediate diaphragms and no formwork in the field, which can accelerate the construction process. However, as a newly developed bridge beam section, the calculation of live load distribution factors (LLDFs) for shear force in the NEXT beam bridges have not been addressed in the current LRFD Specifications. This paper evaluated the LLDFs for shear force in the NEXT beam bridges by using finite element (FE) simulations. The FE models were verified first, followed by a parametric study on the types of NEXT Beam sections and bridge span lengths. Bridges with 8ft-wide and 12ft-wide NEXT beams were explored. The FE results were compared to the LRFD-based LLDFs for recommendations, which could be a good source/reference for future update of NEXT beam bridges in the AASHTO LRFD specifications.

Keywords: Finite Element (FE), Live Load Distribution Factor, NEXT Beam, Shear.

INTRODUCTION

The northeast extreme tee (NEXT) beam sections gained popularity in medium-span bridges in the past few years due to several advantages over the existing beam sections, e.g. box beams and I-shaped beams, including (1) no intermediate diaphragms; (2) no installation or stripping of formwork in the field, which can accelerate the construction process¹. Also, for a NEXT type F beam bridge, the 8-in reinforced concrete deck can protect the NEXT beams from environmental attacks, leading to a good durability of the bridge system^{1,2}. In past years, the PCI northeast bridge technical committee developed a guideline for using the NEXT beams². Eight different cross sections with different beam depths and beam widths were proposed in the guideline, as shown in Figure 1^{1,2}.

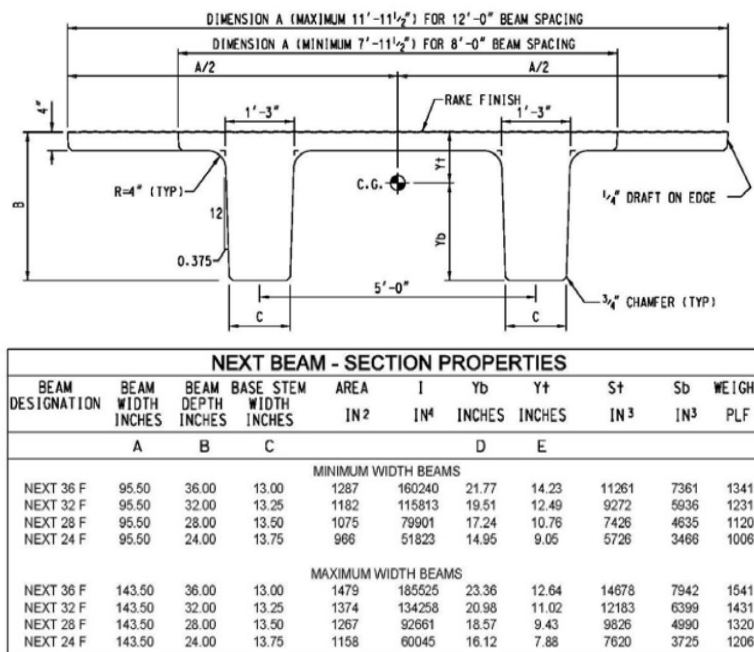


Fig. 1 Section Properties of NEXT type F Beams^{1,2}

It can be seen from Figure 1, the beam width varies from 8 ft to 12 ft, while the section depth varies from 24 in. to 36 in. For all the beam sections above, the spacing between the two stems is 5 ft on centers. Thus, the 8 ft wide and 12 ft wide NEXT beams give a 1.5 ft and 3.5 ft wide top overhang flange, respectively, which leads to an uneven stem spacing in a bridge with more than one NEXT beam. Note that, in the AASHTO LRFD design specifications³, the equations for calculating live load distributions factors (LLDF) for moments and shear forces only valid for bridges with an even girder spacing³. In this regard, the AASHTO equations for LLDFs cannot be directly applied to the NEXT beam bridges. Also, in the current AASHTO LRFD Specifications³, the NEXT beam sections have not been included³.

In recent years, several researches have been conducted for assessing the LLDFs for moments in NEXT beam bridges^{4,5,7}. Huang and Strazar (2014)⁴ employed 3-D finite element (FE) simulations to evaluate the live load distribution for moments in NEXT beam bridges. The results indicated that using the AASHTO type “k” LLDFs for moment for interior beams could lead to a safe design of bridges with 8ft-wide NEXT beams⁴. However, bridges with 12ft wide NEXT beams were not studied in that paper. Bajhat et al. (2014) reported an evaluation of moment LLDFs for a NEXT beam bridge through field load testing and finite element modeling, which indicated using an average stem spacing can lead to a safe design for moments⁷. Huang and Davis (2016)⁵ investigated skew correction factors for live load distribution for moment in NEXT beam bridges by using FE simulations. The results indicated that the skew correction factors from FE simulations had an excellent agreement with that calculated from the LRFD equations⁵. To date, the study on LLDFs for shear force in NEXT beam bridges is limited and more research shall be executed. Therefore, this paper intended to evaluate the LLDFs for shear force in simple span NEXT beam bridges by FE simulations. For convenience, the reactions were used to determine the LLDFs for shear in this paper.

VERIFICATION OF FINITE ELEMENT MODELING

Two dimensional (2-D) FE modeling of bridges has been indicated to have comparable accuracies by several researchers, e.g. Hayes, et al. (1986)⁸; Dicleli and Erhan (2009)⁹. In this study, a 2-D FE modeling was employed to investigate the LLDFs for shear force in NEXT beam bridges by using CSiBridge program⁶. A total of eight one-beam bridges were simulated in CSiBridge and the FE results were verified by manual solutions. Each NEXT beam bridge was modeled by beam elements with 6 degrees of freedom at each node, whereas shell elements were employed to model the 8 in. thick bridge deck^{6,9}. When modeling the NEXT beam, two beam lines were used to simulate each beam stem, in which a half section of the NEXT beam was assigned to each beam line. Table 1 showed the beam sections and bridge span lengths of these one-beam bridges.

Table 1 Summary of the eight one-beam bridges

Section	8 ft wide beam				12 ft wide beam			
	NEXT 32F		NEXT 36F		NEXT 32F		NEXT 36F	
Length	66.7 ft	79 ft	80 ft	85 ft	58 ft	66.7 ft	68 ft	74 ft

Concrete compressive strengths for the NEXT beam and concrete deck were assumed as of 8.0 ksi and 4.0 ksi, respectively. The AASHTO LRFD design loading³ (i.e., HL-93) was assigned on the one-beam bridge model to obtain the structural response, i.e., reactions, per lane loading. Note that the HL-93 loading consists of a design truck, HS-20, and a 0.64 k/ft design lane load³. In the FE models, the design truck with a 33% dynamic impact³ was mimicked as six point loads, as shown in Fig. 2, while the design lane load was uniformly distributed as a pressure load over the entire beam. Under the HL-93 loading, the stem

reactions were obtained for the one-beam bridge, as shown in Fig. 3 (NEXT 32F, 66.7 ft long). Note that the two stem reactions were the same in a NEXT beam because of the symmetry of the beam section.

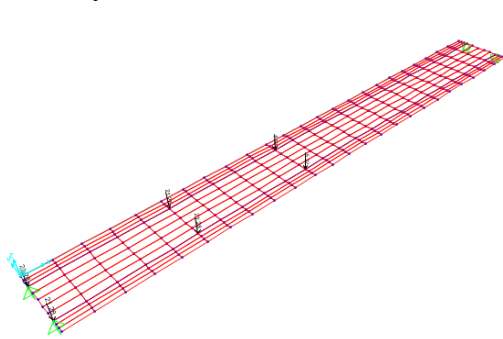


Fig. 2 AASHTO design ruck load (mimicked as 6 point loads)

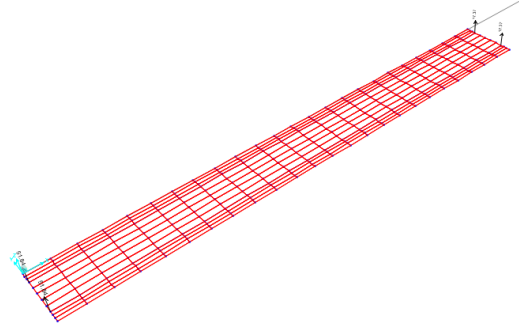


Fig. 3 Reactions under HL-93 loading

Fig. 4 summarized the maximum stem reactions under HL-93 loading for all the eight bridges being investigated. Fig. 4 also showed the load configuration³ (before applying the dynamic impact) for computing the manual solution of the maximum support reaction. Half of the reaction at support “A” was used for the comparison with the corresponding FE stem reaction.

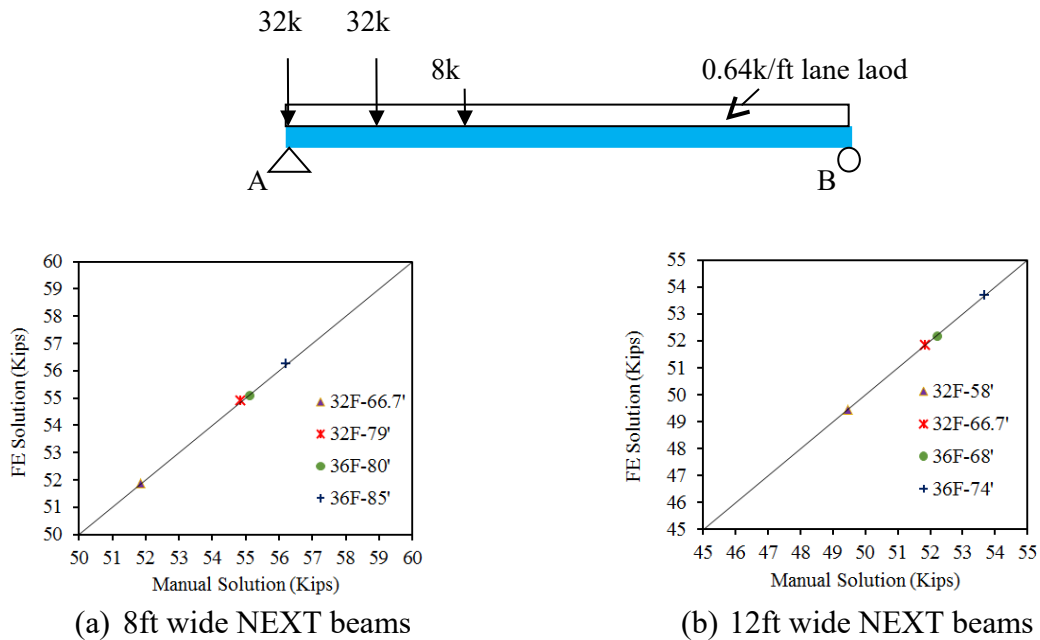


Fig. 4 Comparisons of max. stem reactions from FE solutions and Manual solutions

As can be seen, the differences between the FE results and manual solutions are minimal (less than 0.5%), which indicated the FE modeling by CSiBridge⁶ can achieve an excellent accuracy in capturing the structural responses of NEXT beam bridges. Therefore, CSiBridge⁶ was employed for FE simulations of NEXT beam bridges in this study, as discussed below.

LIVE LOAD SIMULATIONS OF FULL BRIDGES BY FINITE ELEMENT

A total of eight NEXT beam full bridges were simulated in this study. Two typical bridge sections were selected from Culmo and Seraderian (2010)¹, as shown in Table 2.

Table 2 Summary of the eight simulated NEXT bridges

	Type I: four 8 ft wide beams				Type II: three 12 ft wide beams			
	<p>(Beam section adapted from Ref [2])</p>				<p>(Beam section adapted from Ref [2])</p>			
Section	NEXT 32F		NEXT 36F		NEXT 32F		NEXT 36F	
Length	66.7 ft	79 ft	80 ft	85 ft	58 ft	66.7 ft	68 ft	74 ft

One Design Lane Loaded Cases

Fig. 5 shows a 66.7 ft long bridge with four 32F NEXT beams (8 stems) with one design lane loaded, which was placed right next to the left curb^{3,4,5} (designated as case 1-1). This case scenario can give the maximum loading effects on the exterior beam. The HL-93 loading was simulated as a moving load within the design lane in CSiBridge⁶. In order to determine the maximum loading effect on the interior beams, additional load cases were investigated by moving the load case 1-1 transversely by one foot increments to the right curb direction. Once the center of the loaded lane reached the centerline of the bridge cross section, the load case was terminated due to the symmetry of the bridge. After running the analysis, the maximum reactions at each stem end were obtained for each one-lane loaded case. Fig. 6 showed the reactions of the NEXT 32F beam bridge under different load cases. Due to the symmetry of the bridge, only the first four stem reactions were plotted.

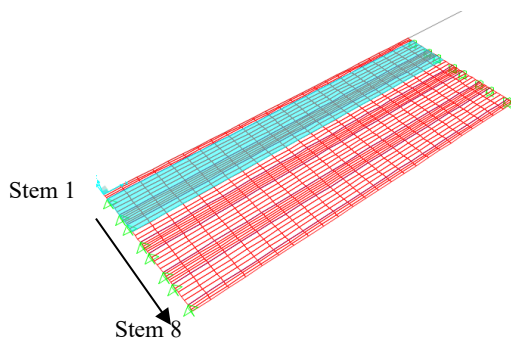


Fig. 5 Loading profile for Case 1-1

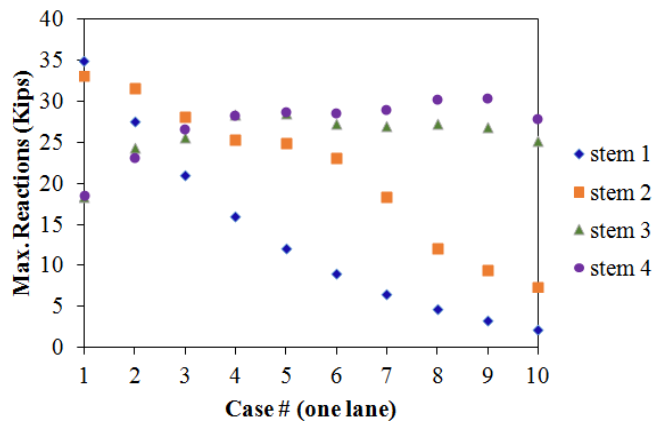


Fig. 6 Maximum reactions under one lane loaded cases

As can be seen, for the exterior beam, the maximum reaction was 34.93 kips located at stem 1. From the FE verification part in this paper, it can be seen that the reaction per lane loading for each stem was 51.84 kips. Therefore, the LLDF for shear force in exterior beam under one lane-loaded case can be determined as equal to $1.2 \cdot 34.93 / 51.84 = 0.809$. Note that, in accordance with the AASHTO LRFD specifications³, a multiple presence factor of 1.2 shall be applied to the one-lane loaded case³. For the interior beam, the maximum reaction was 30.45 kips located at stem 4, giving a LLDF for shear force equal to $1.2 \cdot 30.45 / 51.84 = 0.705$. By repeating the above study, LLDFs for shear force in other NEXT beam bridges can be determined for the one lane loaded cases, as can be seen in Figures 11-14.

Two Design Lane Loaded Cases

Fig.7 shows the 66.7ft long 32F NEXT beam bridge with two adjacent design lanes loaded, which were placed right next to the left curb^{3,4,5} (designated as case 2-1). This case scenario can give the maximum loading effects on the exterior beam. The HL-93 loading was simulated as a moving load within the design lane⁶. In order to determine the maximum loading effect on the interior beams, additional load cases were investigated by moving the load case 2-1 transversely by one foot increments to the right curb direction. Similar to the one lane loaded cases, once the center of the loaded lane reached the centerline of the bridge cross section, the load case was terminated due to the symmetry of the bridge. As stated in AASHTO LRFD specification³, the design lane load can appear anywhere within the 12 ft traffic lane³. In this sense, another load profile (designated as case 2-7) was also used for further study, as shown in Fig. 8. By moving load case 2-7 transversely can give more critical loading effects on the interior beams. A total of 6 cases were explored by moving the case 2-7 transversely to the right in one foot increments. After running the analysis in CSiBridge, the maximum reactions at each stem were obtained for each two-lane loaded case. Fig. 9 showed the maximum reactions for the NEXT 32F beam bridge. Due to the symmetry of the bridge, only the first four stem reactions were plotted.

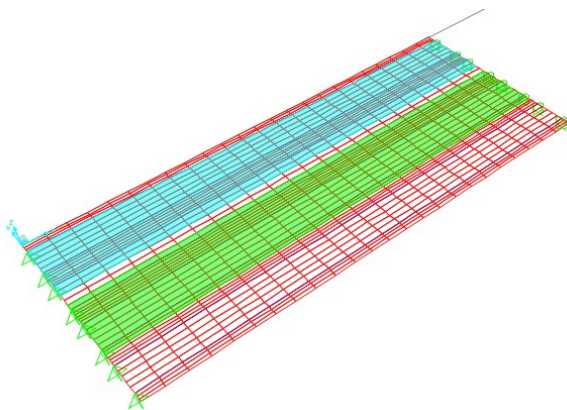


Fig. 7 Loading profile for Case 2-1

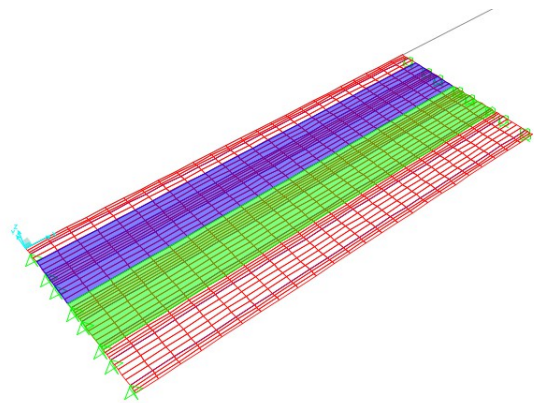


Fig. 8 Loading profile for Case 2-7

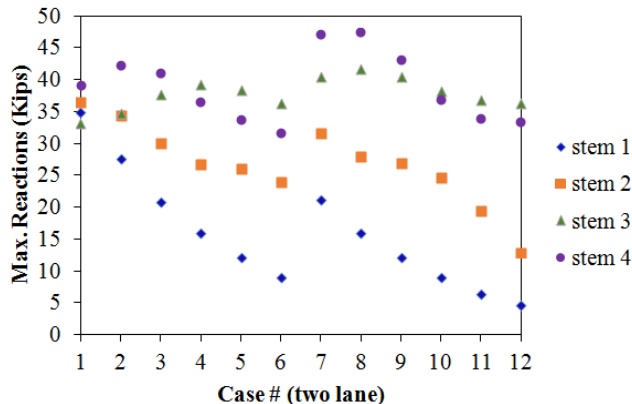


Fig. 9 Maximum reactions under two lane loaded cases

As can be seen, for the exterior beam the maximum reaction was 36.70 kips located at stem 2. The reaction per lane loading for each stem is 51.84 kips. Thus, the LLDF for shear force in exterior beam under the two-lane loaded case can be determined as equal to $36.70/51.84=0.708$. Note that, per AASHTO LRFD specifications³, a multiple presence factor of 1.0 shall be applied to the two lane loaded case³. For the interior beam, the maximum reaction was 47.50 kips located at stem 4, giving a LLDF for shear force equal to $47.50/51.84=0.916$. By repeating the above procedure, LLDFs for shear force in other NEXT beam bridges can be determined for the two lane loaded cases, as can be seen in Figures 11-14.

SHEAR DISTRIBUTION FACTOR IN THE AASHTO LRFD SPECIFICATIONS

In accordance with the AASHTO LRFD Bridge Design Specifications, *Table 4.6.2.2.3a-1—Distribution of Live Load per Lane for Shear in Interior Beams*³, the LLDFs for shear in interior beams (type k) shall be computed with the following equations³:

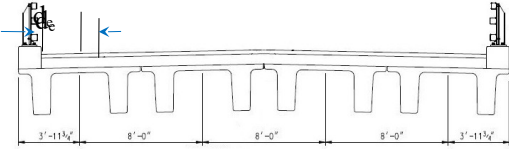
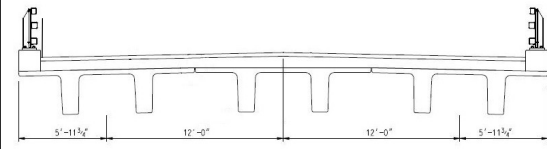
Nb=3	One-lane loaded	Lever rule
	Two and more lanes loaded	Lever rule
Nb≥4	One-lane loaded	$DFV^{i,1}=0.36+S/25$
	Two and more lanes loaded	$DFV^{i,2+}=0.2+S/12-(S/35)^2$ (S= beam spacing)

This paper intended to examine the suitability of using the AASHTO type “k” LLDF equations for the NEXT beam bridges. In this sense, for type I bridges (i.e., four 8 ft wide beams), S=8 ft, whereas S=12 ft was used for type II bridges (i.e., three 12 ft wide beams).

For exterior beams, the LLDFs for shear shall be computed in accordance with AASHTO LRFD *Table 4.6.2.2.3b-1*³, as follows:

One-lane loaded	Lever rule	
Two and more lanes loaded	DFV _{e,2+} = e _v × DFV _{i,2+} e _v = 0.6 + de/10	Nb ≥ 4
	Lever rule	Nb = 3

Where, de = horizontal distance from the centerline of the exterior web of exterior beam at the deck level to the interior edge of curb or traffic barrier³. The following illustrated the “de” for type I and type II bridges.

Type I : de = 3.98ft - 1.5ft = 2.48ft	Type II : de = 5.98ft - 1.5ft = 4.48ft
 <p>(Beam section adapted from Ref [2])</p>	 <p>(Beam section adapted from Ref [2])</p>

With the discussions above, the LLDFs for shear force were calculated for all the eight bridges being investigated, for both one lane and two lane loaded cases. Figures 11-14 showed the comparisons of the LLDFs for shear between the FE and LRFD results.

As can be seen from Fig. 11, the FE results had an excellent agreement with that from LRFD for both one lane and two lane loaded cases, which indicated the AASHTO LLDF equations can be applied to the exterior beam design in the bridges with 8ft wide NEXT beams. Fig. 12 showed the LLDFs for shear force in exterior beam in bridges with 12 ft wide NEXT beams. As can be seen, only for the two-lane loaded case FE results agreed well with the LRFD’s, whereas for the one lane loaded case FE results is larger than that from LRFD by approximately 15%.

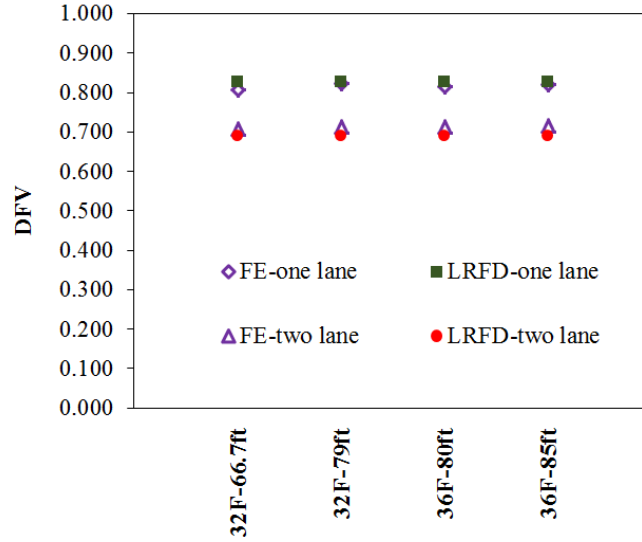


Fig. 11 DFV for exterior beam (8 ft wide Next Beam bridge)
 Note: DFV=distribution factor for shear force

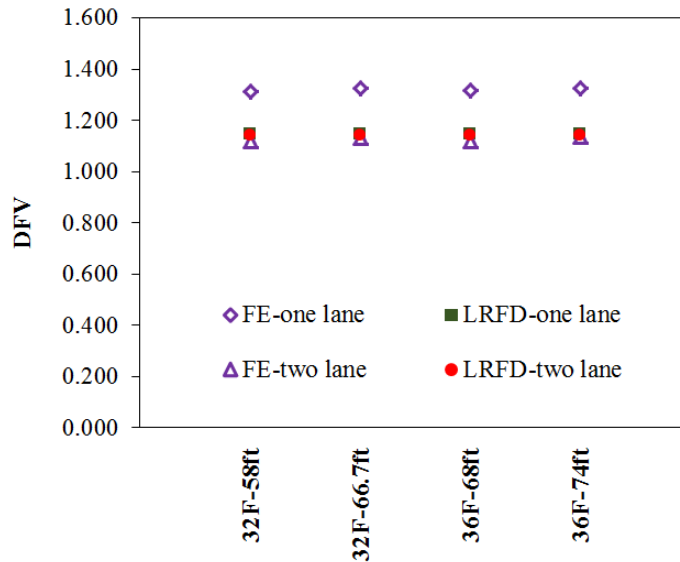


Fig. 12 DFV for exterior beam (12 ft wide Next Beam bridge)

The LLDFs for shear in interior beams, as computed from the FE results and the LRFD equations, were plotted in Fig. 13 and Fig. 14 for bridges with 8 ft wide and 12 ft wide NEXT beams, respectively. As can be seen, for the bridges with 8ft wide NEXT beams, the LRFD and FE results had an excellent agreement of LLDFs for shear under the one lane loaded cases, whereas for the two lane loaded cases, the FE results were 10-12.5% higher than that from LRFD equations. From Figure 14, it can be seen that: the FE results from one lane loaded cases exhibited a 7-9% higher LLDFs than that from LRFD equations, whereas the FE results were 3-5% higher than that from LRFD equations for the two lane loaded cases.

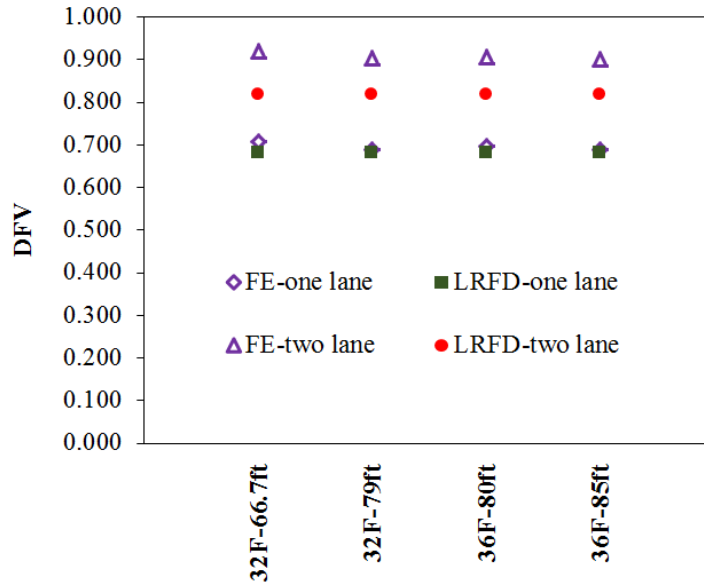


Fig. 13 DFV for interior beam (8 ft wide Next Beam bridge)

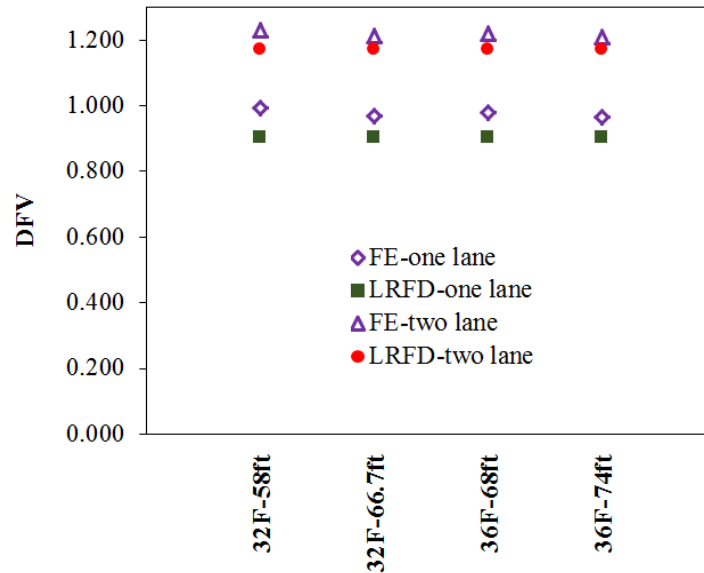


Fig. 14 DFV for interior beam (12 ft wide Next Beam bridge)

It can also be observed that, for all the eight bridges being explored, the FE and LRFD gave the same trend for LLDFs for shear force, that is, the LLDFs for shear forces only depend on the girder spacing. The girder section type and bridge span length had minimal effects on the LLDFs for shear force in NEXT beam bridges.

CONCLUSIONS

In this paper, the LLDFs for shear force in NEXT beam bridges were investigated by finite element (FE) simulations. Bridges with 8ft-wide and 12ft-wide NEXT beams were explored. The FE results were compared to the manual solutions as computed with the AASHTO LRFD equations. Based on the study in this paper, the following conclusions can be made.

- For bridges with 8 ft wide NEXT beams:
 - for exterior beams, the FE results had an excellent agreement with the LRFD results for both one lane and two lane loaded cases
 - for interior beams, the FE results had an excellent agreement with the LRFD results for one lane loaded cases; whereas, for two lane loaded case the FE results gave a higher LLDFs for shear than that from LRFD, by approximately 10-12.5% .
- For bridges with 12 ft wide NEXT beams:
 - for exterior beams, the FE results had an excellent agreement with the LRFD results for two lane loaded cases, whereas, for one lane loaded cases FE gave higher LLDFs for shear than that from LRFD by approximately 15%,
 - for interior beams, the FE results were slightly higher than that from LRFD: approximately 3-5% for two lane loaded cases and 7-9% for one lane loaded cases.
- The FE gave the same trend for LLDFs for shear as that from LRFD equations, which depend on the girder spacing. The girder section type and bridge span length had minimal effects on the LLDFs for shear force in NEXT beam bridges.

The above conclusions were made on the basis of a limited number of bridge cases. Further studies on other parameters, including but not limited to other NEXT beam sections, number of beams in a bridge, and skew effects, are under investigation by the author.

REFERENCES

1. Culmo, M.P., and Seraderian, R.L. (2010), Development of the northeast extreme tee (NEXT) beam for accelerated bridge construction, *PCI Journal* 55(3), 86-101.
2. Guidelines for Northeast Extreme Tee Beam (NEXT beam), First Edition, PCI Northeast, 2012, pp64.
3. AASHTO LRFD Bridge Design Specifications (2014), 7th Edition, The American Association of State Highway and Transportation Officials, Washington, D.C.
4. Huang, J. and Strazar, C., Evaluation of live load distribution factor for NEXT beam bridge, Proceedings of the 2014 PCI Annual Convention an Exhibition and National Bridge Conference, Washington, D.C., Sept. 6-9, 2014.
5. Huang, J. and Davis, J., Skew Correction Factor for Bending Moment in Next Beam Bridges, Proceedings of 2016 PCI Convention and National Bridge Conference, Nashville, Tennessee, USA, March 3-6, 2016.
6. CSi Analysis Reference Manual (2015), Computers and Structures Inc., CA, USA.
7. Bahjat, R., et al., Evaluation of moment live load distribution of a NEXT F beam bridge through field load testing and FE modeling, Proceedings of the 2014 PCI Annual Convention an Exhibition and National Bridge Conference, Washington, D.C., Sept. 6-9, 2014.
8. Hays, C. O., Sessions, L. M., and Berry, A. J. (1986), Further studies on lateral load distribution using a finite element method (No. 1072), Transportation research board, Washington, D.C.
9. Dicleli, M., & Erhan, S. (2009), Live load distribution formulas for single-span prestressed concrete integral abutment bridge girders, *Journal of Bridge Engineering*, 14(6), 472-486.